Frequency Response Properties of Forced Climatic SST Anomaly Variability in the North Atlantic

GEORGE R. HALLIWELL JR.

MPO/RSMAS, University of Miami, Miami, Florida

DENNIS A. MAYER

Physical Oceanography Division, NOAA/AOML, Miami, Florida

(Manuscript received 24 April 1995, in final form 21 May 1996)

ABSTRACT

Frequency response properties of North Atlantic (5°–57°N) sea surface temperature anomaly (T_{sa}) variability with periods of several months to 20 years are characterized using the Comprehensive Ocean–Atmosphere Data Set (COADS). Significant direct forcing of T_{sa} variability by the anomalous wind field (primarily through the resulting anomalous surface turbulent heat flux) is observed in the westerly wind and trade wind belts. To characterize properties of the large-scale climatic T_{sa} response to this forcing over the entire frequency band resolved, it is necessary to consider the dual role of anomalous surface heat flux as both the dominant local forcing mechanism and the dominant damping mechanism, the latter through a negative linear feedback (Newtonian relaxation). At frequencies where wind forcing is important, good agreement exists between the frequency response function estimated from data and the same function theoretically predicted by a simple stochastic forcing model where the locally forced response is damped by a negative linear feedback with a decay time scale of 3 mo. To make this comparison, the total anomalous surface heat flux represented by the standard bulk formula was decomposed into two components, one primarily representing the local wind forcing and the other primarily representing negative feedback damping. In the westerlies, wind forcing is effective over periods from several months to 8 yr, primarily 2–4 yr, and is ineffective at periods of 8–20 yr. These fluctuations are primarily forced in the western part of the basin then propagate to the east and northeast across the Atlantic at a characteristic speed of 6 km day^{-1}. When time series of winter-only T_{sa} are analyzed, however, wind forcing of winter to winter T_{sa} variability remains significant at decadal and longer periods. In the trades, wind forcing is effective over periods from 8 mo to 13.3 yr, primarily 2–3 yr and 7–13.3 yr, and significant seasonal differences are not observed.

1. Introduction

There has been increasing effort in recent years to understand the physical processes controlling sea surface temperature (T_s) variability in the Atlantic Ocean because of its key role in coupling the ocean–atmosphere system at climatic timescales (scales exceeding those of synoptic atmospheric systems). It is difficult to diagnose the physical processes driving the anomalous variability of T_s about the climatological mean annual cycle (T_{sa}) given the complex coupled nature of the ocean–atmosphere system. At climatic timescales, anomalous atmospheric patterns influence T_{sa} through the resulting anomalous patterns of local air–sea fluxes (including the influence of ageostrophic Ekman flow driven by the momentum flux) and through the near-surface oceanic flow field (both wind-driven and thermohaline) driven nonlocally by the atmosphere. Identification of forcing mechanisms is difficult because anomalous T_{sa} patterns can drive anomalous atmospheric patterns (e.g., Folland et al. 1986; Lau and Nath 1990) that then act to modify both the anomalous air–sea flux and oceanic flow patterns that force T_{sa}.

Despite these difficulties, a number of studies have successfully characterized important properties of forced climatic T_{sa} variability at large scales (scales exceeding those of synoptic ocean eddies) in the Atlantic Ocean. Bjerknes (1964) hypothesized that North Atlantic T_{sa} variability responds primarily to changes in the oceanic flow field at periods exceeding decadal and responds primarily to local thermodynamical forcing at shorter interannual periods. This hypotheses has been supported by recent analyses of T_s fields from the Comprehensive Ocean–Atmosphere Data Set (COADS; Woodruff et al. 1987) for the subtropical and subpolar North Atlantic (e.g., Deser and Blackmon 1993; Kushnir 1994). Bjerknes (1964) demonstrated that large-scale patterns of T_s change from the late 1890s to the early 1920s and from the early 1920s to

Corresponding author address: Dr. George R. Halliwell, RSMAS/MPO, University of Miami, 4600 Rickenbacker Causeway, Miami, FL 33149-1098.

the late 1930s were consistent with patterns expected to be caused by changes in the large-scale oceanic flow field and were apparently not associated with local changes in air–sea fluxes. Furthermore, Kushnir (1994) compared the pattern of T_s change between 1950–64 and 1970–84 average maps to results from the numerical modeling study of Delworth et al. (1993) and noted that the observed pattern of T_s change in the North Atlantic Westerly Wind belt resembled the pattern caused by changes of the thermohaline meridional overturning circulation (MOC) in the model ocean. At shorter interannual timescales, however, local anomalous surface turbulent heat flux forcing due in large part to the anomalous wind speed pattern is important in the North Atlantic (e.g., Bjerknes 1964; Frankignoul 1985; Cayan 1992a, 1992b; Zorita et al. 1992; Luksch and von Storch 1993; Deser and Blackmon 1993; Kushnir 1994).

Although the earlier studies demonstrated that the relative importance of these forcing mechanisms depends on frequency, they did not provide a detailed accounting of how the relative importance of local and oceanic forcing changes as a function of frequency. It is important to improve our understanding of this frequency dependence in different regions of the North Atlantic for a number of reasons. It will shed light on how the atmosphere and ocean are coupled at different frequencies and can be useful in evaluating the performance of coupled ocean–atmosphere models. Identification of frequency bands where T_{sa} is primarily driven by local thermodynamical fluxes is tantamount to identifying frequency bands where the atmosphere predominantly acts to thermodynamically force the ocean. In contrast, the ocean may predominantly act to thermodynamically force the atmosphere in frequency bands where T_{sa} responds primarily to oceanic flow variability. At lower frequencies where forcing by oceanic flow variability (including the MOC) is expected to be important, the T_{sa} variability that is locally forced by air–sea fluxes must be accounted for to unambiguously identify T_{sa} variability driven by the ocean.

Although oceanic flow data were not available for the present study, progress in understanding the frequency dependence of ocean–atmosphere coupling can be made by studying the frequency response properties of T_{sa} variability with respect to local forcing alone. We therefore present an analysis of the T_{sa} response to local forcing in the North Atlantic Ocean, focusing on variability with periods between six months and two decades. We characterize frequency response properties in both the westerly wind and trade wind belts and identify frequency bands where local forcing is dominant, significant but not dominant, and insignificant. The theoretical framework guiding the analysis is provided by a simple linearized slab mixed-layer anomalous temperature balance [the stochastic forcing model of Frankignoul and Hasselmann (1977)] where T_{sa} is driven by a local forcing term and damped by a negative feedback term (Newtonian relaxation to $T_{sa} = 0$). This model is used to predict the frequency response properties of locally forced T_{sa} variability for comparison to the observed response properties. To estimate frequency response properties from observations, we focus exclusively on the response to anomalous surface turbulent (latent plus sensible) heat flux forcing arising from the anomalous wind speed pattern. Cross spectrum analysis between T_{sa} and this local wind forcing is performed to characterize observed frequency response properties and to demonstrate that they are in good agreement with properties predicted by the stochastic model.

2. Predicted frequency response properties

We consider the local slab mixed-layer temperature balance with horizontal advection and diffusion neglected. To obtain the anomalous temperature balance, T_s (assumed to equal bulk mixed-layer temperature) is decomposed into climatological mean annual cycle and anomaly components ($T_s = T_s^* + T_{sa}$). Here T_{sa} varies in response to the anomalous vertical divergence of vertical heat flux (F):

$$\frac{\partial T_{sa}}{\partial t} = F. \tag{1}$$

The influence of Ekman flow is neglected because it is smaller by a factor of 2–4 than anomalous surface heat flux forcing at the subtropical and subpolar latitudes considered in the present study (e.g., Haney 1985). Horizontal diffusion was neglected in anticipation of the dominant role of negative feedback damping for large-scale climatic T_{sa} variability (e.g., Reynolds 1979; Frankignoul and Reynolds 1983).

Derivation of the stochastic forcing model where local forcing is damped by a negative linear feedback is presented in Frankignoul (1979, 1985) and is briefly summarized here. We note that F depends in part on T_{sa} and assume that $\langle F \rangle = 0$ for $T_{sa} = 0$, where angle brackets denote an ensemble average over many realizations of F. A single realization of F is then given by

$$F = \langle F \rangle + F_a. \tag{2}$$

Expanding F with respect to T_{sa} and truncating to first order, we obtain

$$F = F_a + \left.\frac{\partial \langle F \rangle}{\partial T_{sa}}\right|_{T_{sa}=0} T_{sa}. \tag{3}$$

Defining λ as the negative of the partial derivative in (3), the desired temperature balance is

$$\frac{\partial T_{sa}}{\partial t} = F_a - \lambda T_{sa}, \tag{4}$$

where λ^{-1} can be interpreted as a decay timescale that has a typical value of about three months for the North

Atlantic (e.g., Reynolds 1979). The stochastic model (4) has been used to quantify properties of the T_{sa} response at climatic timescales with respect to local forcing by unresolved synoptic atmospheric variability in midlatitudes (e.g., Frankignoul and Hasselmann 1977; Frankignoul 1979; Frankignoul and Reynolds 1983). The unresolved synoptic variability was assumed to result in a white-noise spectrum of F (random forcing) at climatic timescales. Given this assumption, (4) successfully predicts the magnitude and shape of the observed T_{sa} autospectrum in regions away from strong mean flow as long as variability forced by ocean eddies has been filtered out.

Most earlier studies that characterized the relationship between T_{sa} and local forcing F_a have considered the form of the cross-correlation function predicted by (4) (e.g., Frankignoul 1985). Since our interest is in the frequency dependence of this relationship, we will compare the frequency response (transfer) function of T_{sa} with respect to F_a estimated from observations to the function predicted by (4). Frequency dependence in response properties arises because the relative magnitude of the time derivative and damping terms of (4) depends on frequency (e.g., Frankignoul 1979, 1995). At periods much shorter than the decay timescale λ^{-1}, the damping term is much smaller than the time derivative term so (4) can be approximated by

$$\frac{\partial T_{sa}}{\partial t} \approx F_a. \tag{5}$$

Term $\partial T_{sa}/\partial t$ is therefore in-phase with F_a. At periods much longer than the decay timescale, the time derivative term is much smaller than the damping term so (4) can be approximated by the quasi-steady balance

$$T_{sa} \approx \lambda^{-1} F_a. \tag{6}$$

Here T_{sa} is therefore in phase with F_a, while the response amplitude is limited by the damping to roughly equal λ^{-1} times the magnitude of F_a fluctuations.

This asymptotic behavior is contained in the frequency response function predicted by (4), the gain and phase of which are

$$|H(\omega)| = (\omega^2 + \lambda^2)^{-1/2} \tag{7}$$

and

$$\phi(\omega) = -\tan^{-1}(\omega/\lambda), \tag{8}$$

where $H(\omega)$ is the frequency response function and ω is frequency. The gain and phase functions plotted in Fig. 1 were calculated for a range of periods from 1 mo–50 yr assuming $\lambda^{-1} = 3$ mo. For a given magnitude of local forcing, (7) predicts that the amplitude of the T_{sa} response increases with decreasing frequency, asymptotically approaching a maximum of λ^{-1} times the magnitude of F_a fluctuations as predicted by (6). At a period of 1 yr (6 mo), the response amplitude is one-half (30%) of this maximum. The phase from (8) is nearly zero at decadal and longer periods, while the phase is close to −90 at periods less than 3 mo (F_a is nearly in-phase with $\partial T_{sa}/\partial t$). The phase is −45° at a period of 1.5 yr (2π times the decay timescale λ^{-1}). The resulting lag time of T_{sa} with respect to F_a is small at short periods and asymptotically approaches a maximum value of λ^{-1} (3 mo) at long periods (not shown).

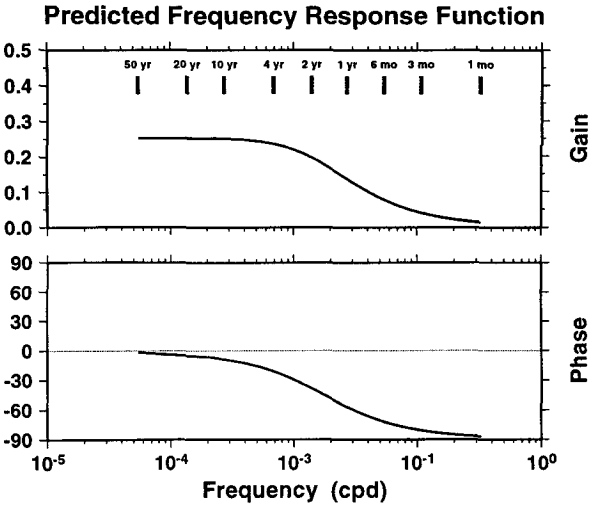

FIG. 1. The gain function predicted by (7) (top) and the phase function in degrees predicted by (8) (bottom). The gain function provides the response amplitude in degrees Celsius for a forcing magnitude of 1°C yr^{-1}, so it asymptotically approaches λ^{-1} (0.25 yr) as frequency approaches zero.

Using observations from ocean station P, Frankignoul (1979) calculated the frequency-dependent phase lag of T_{sa} with respect to forcing represented by the total anomalous surface turbulent heat flux term of the mixed-layer temperature balance, resolving periods ranging from 12 h to about 3 yr. The present study extends these earlier results by resolving periods up to 20 yr, by including a comparison between observed and predicted gain and by documenting regional differences between the westerly wind and trade wind belts. We also demonstrate the necessity of decomposing the anomalous heat flux term into forcing and feedback components to properly characterize frequency response properties at the longer periods resolved.

3. Observed frequency response properties

a. Estimation of terms of the stochastic model (4)

Earlier studies (e.g., Frankignoul and Reynolds 1983; Haney 1985) have demonstrated that anomalous surface turbulent heat flux exerts the dominant influence on large-scale climatic T_{sa} variability at subtropical and subpolar latitudes. Furthermore, Frankignoul (1979, 1985, 1995) has pointed out that this flux acts not only to force T_{sa} but also makes the dominant contribution to the negative feedback that dampens the

forced variability. We will therefore decompose the anomalous surface heat flux term in the anomalous mixed-layer temperature balance into two terms that approximately represent the forcing and feedback terms of the stochastic model. Time series of these terms will be estimated from observations and used to calculate the observed frequency response properties.

To obtain the anomalous temperature balance, we first define a positive total surface turbulent heat flux (Q_T) to be upward (representing the ocean losing heat to the atmosphere). The bulk formula representation is then

$$Q_T = \rho_A C_L L W \Delta q + \rho_A C_S W \Delta T + S, \quad (9a)$$

where

$$\Delta q = q_s - q_A, \quad (9b)$$

$$\Delta T = T_s - T_A, \quad (9c)$$

and where subscript T signifies turbulent, ρ_A is surface atmospheric density, C_L and C_S are bulk transfer coefficients that depend on air stability, L is latent heat of evaporation, W is wind speed, T_A is 10-m atmospheric temperature, q_s is surface saturation specific humidity (a function of T_s), and q_A is 10-m atmospheric specific humidity. The term S is included to represent the influence of unresolved synoptic variability through terms involving correlations between synoptic variables. The anomalous flux is derived by decomposing dependent variables in (9) into mean annual cycle and anomaly components, then subtracting all terms that contribute to Q_T^*:

$$Q_{Ta} = \rho_A C_L L (W_a \Delta q^* + W^* \Delta q_a) + \rho_A C_S (W_a \Delta T^* + W^* \Delta T_a) + S_a. \quad (10)$$

Terms involving products of anomaly variables are neglected because they are comparatively small at the long timescales resolved in the present study. Since we assume that Q_{T_a} exerts the dominant influence on T_{sa}, (1) becomes

$$\frac{\partial T_{sa}}{\partial t} \approx F_T, \quad (11a)$$

where

$$F_T = -(\rho_m c_p h^*)^{-1} Q_{T_a}, \quad (11b)$$

and where ρ_m is mixed-layer water density, c_p is specific heat of seawater at constant pressure, and h is mixed-layer thickness. Since anomalous mixed layer thickness h_a is not available from the COADS, we cannot take into account the anomalous thermal inertia of the slab mixed layer resulting from nonzero h_a.

It is not possible to exactly separate F_T into forcing and feedback components. However, a partial separation can be achieved by first considering the terms of F_T obtained from (11b) and (10) that represent anomalous wind speed forcing:

$$F_{T1} = -\rho_A (\rho_m c_p h^*)^{-1} (C_L L W_a \Delta q^* + C_S W_a \Delta T^*). \quad (12)$$

The remaining contribution of F_T is then given by

$$F_{T2} = -\rho_A (\rho_m c_p h^*)^{-1} \times (C_L L W^* \Delta q_a + C_S W^* \Delta T_a) + F_{TS}. \quad (13)$$

Term F_{T2} does contain the negative feedback damping due to its negative linear dependence on q_{sa} and T_{sa}. However, F_{T2} also contains the influence of anomalous atmospheric temperature and humidity variability because it depends in part on q_{Aa} and T_{Aa}. It also contains F_{TS}, the nonlinear influence of unresolved synoptic-scale variability. Despite this complexity, we will demonstrate that F_{T2} does predominantly represent negative feedback damping at interannual periods and that the decomposition (12) and (13) is adequate for the purposes of the present study. This will probably not be true closer to the North American coast where q_{Aa} and T_{Aa} variability will be larger and potentially act as strong forcing mechanisms.

With F_{T1} representing local wind forcing and F_{T2} primarily representing negative feedback damping, the temperature balance (11a) assumes the form of the stochastic model (4):

$$\frac{\partial T_{sa}}{\partial t} \approx F_{T1} + F_{T2}, \quad (14a)$$

where

$$F_{T1} \approx F_a \quad (14b)$$

and

$$F_{T2} \approx -\lambda T_{sa}. \quad (14c)$$

We will estimate F_{T1} and F_{T2} from observations to confirm the hypothesis that (14) is a reasonable approximation to (4) by demonstrating that the following relationships hold. First, from (14c), T_{sa} will be 180° out of phase with F_{T2} at all frequencies if it predominantly represents negative feedback damping. Second, the gain and phase of the observed frequency response function of T_{sa} with respect to F_{T1} calculated using cross spectrum analysis will have the form of the predicted functions (7) and (8).

b. Estimation of F_{T1} and F_{T2}

The observations required to validate the hypothesis that (14) is a reasonable approximation to (4) are primarily obtained from the COADS. Monthly averaged maps of required fields (T_s, W, $W\Delta q$, and $W\Delta T$) were available from the COADS on a 2° latitude–longitude grid. For each field, the monthly maps were averaged over three-month seasons beginning with winter (De-

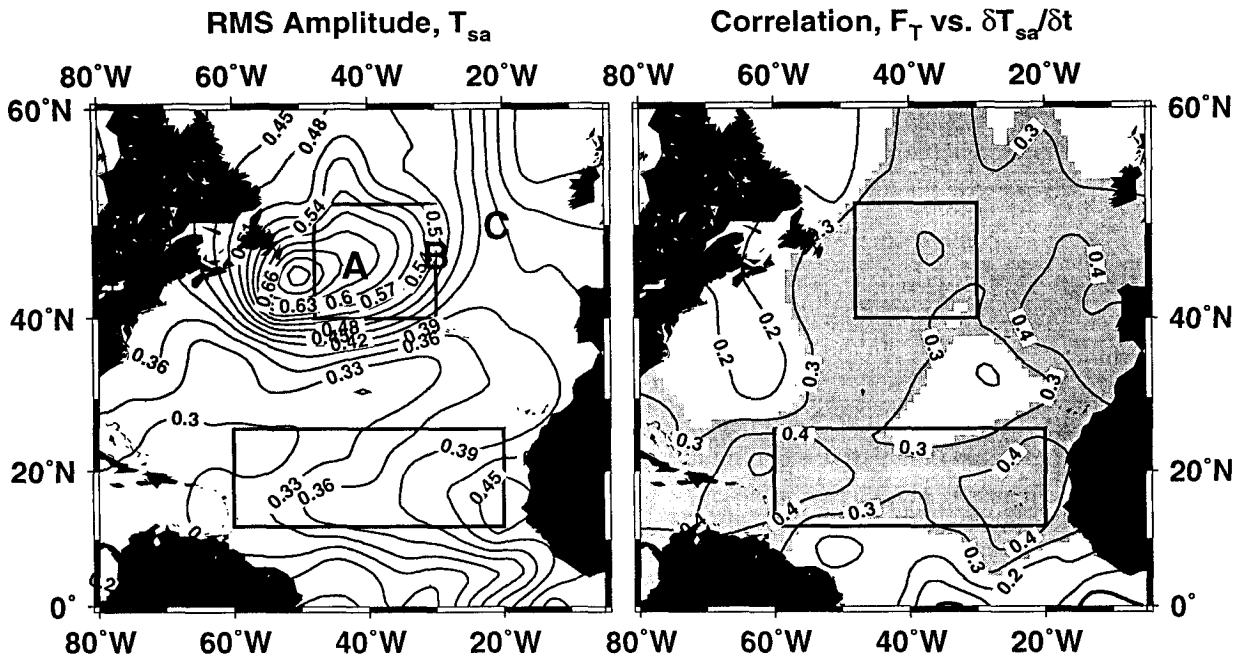

FIG. 2. The temporal rms amplitude of T_{sa} (°C) over all 161 seasons (left) along with maps of the correlation between the terms of (11) (F_T versus $\partial T_{sa}/\partial t$, right). Regions where the correlation coefficient differs significantly from zero with 95% confidence (exceeds 0.28 in magnitude based on 40 effective degrees of freedom in the time series) are shaded. Boxes outline regions where frequency response analyses were performed. Points *A*, *B*, and *C* in the left panel were used for the T_{sa} propagation analysis (Fig. 3).

cember–February) 1948/49 and ending with winter 1987/88, resulting in a time series of 161 seasonal maps. These seasonal fields were used in the analysis of Mayer and Weisberg (1993), who provide further details of the data processing. In addition, maps of Δq^* and ΔT^* were calculated from COADS climatological maps of T_s^*, q_A^*, and T_A^*. The required fields of h^* were obtained from the Lamb (1984) Atlantic seasonal climatology.

To analyze (14), seasonal maps of Q_T were first calculated from (9) using fields of $W\Delta q$ and $W\Delta T$ and constant neutral-stability values for the coefficients C_L and C_S. Term Q_{Ta} in (10) was calculated by removing the mean annual cycle from Q_T and then used to estimate F_T from (11b). Since F_T was calculated from seasonally averaged fields of $W\Delta q$ and $W\Delta T$ derived from individual observations of these products, it does contain the influence of unresolved synoptic variability represented by S_a in (10). Next, fields of W_a were calculated by removing the mean annual cycle from W, then maps of F_{T1} were calculated from (12) using fields of W_a, Δq^*, and ΔT^*. Here F_{T2} was then estimated by subtracting F_{T1} from F_T and hence contains the contribution of unresolved synoptic variability.

Significant errors and biases are present in the COADS dataset (Michaud and Lin 1992). The impact of random errors was reduced in two ways. First, the fields calculated above were further smoothed using a two-dimensional Gaussian filter to represent variability with space scales exceeding several hundred kilometers. In addition to reducing random noise, this smoothing reduces the effects of synoptic eddy "noise" (Frankignoul 1985) while still resolving the dominant large space scales of low-frequency climatic variability in the ocean (Kraus 1982). Second, the local response analysis (section 4) was conducted by estimating observed frequency response functions from autospectra and cross spectra that were ensemble-averaged over regions containing a large number of grid points. To reduce the impact of biases, means and linear trends were removed from all time series analyzed here. Inspection of T_{sa} time series revealed that observed fluctuations with 20–40-yr periods were not artificially removed by this process.

c. *Selection of analysis regions*

For the present study, we consider only the interior North Atlantic between 5° and 57°N, further deleting the immediate Gulf Stream region west of 50°W and the slope water region to the north to focus on the open ocean away from coastal boundary currents. Maps of the rms amplitude of T_{sa} and the correlation between the terms of (11) (Fig. 2) were used to select two regions within this domain to be analyzed. Since the largest T_{sa} variability in the interior Atlantic between 5° and 57°N is found in the westerly wind and trade wind belts, we perform frequency response analyses for

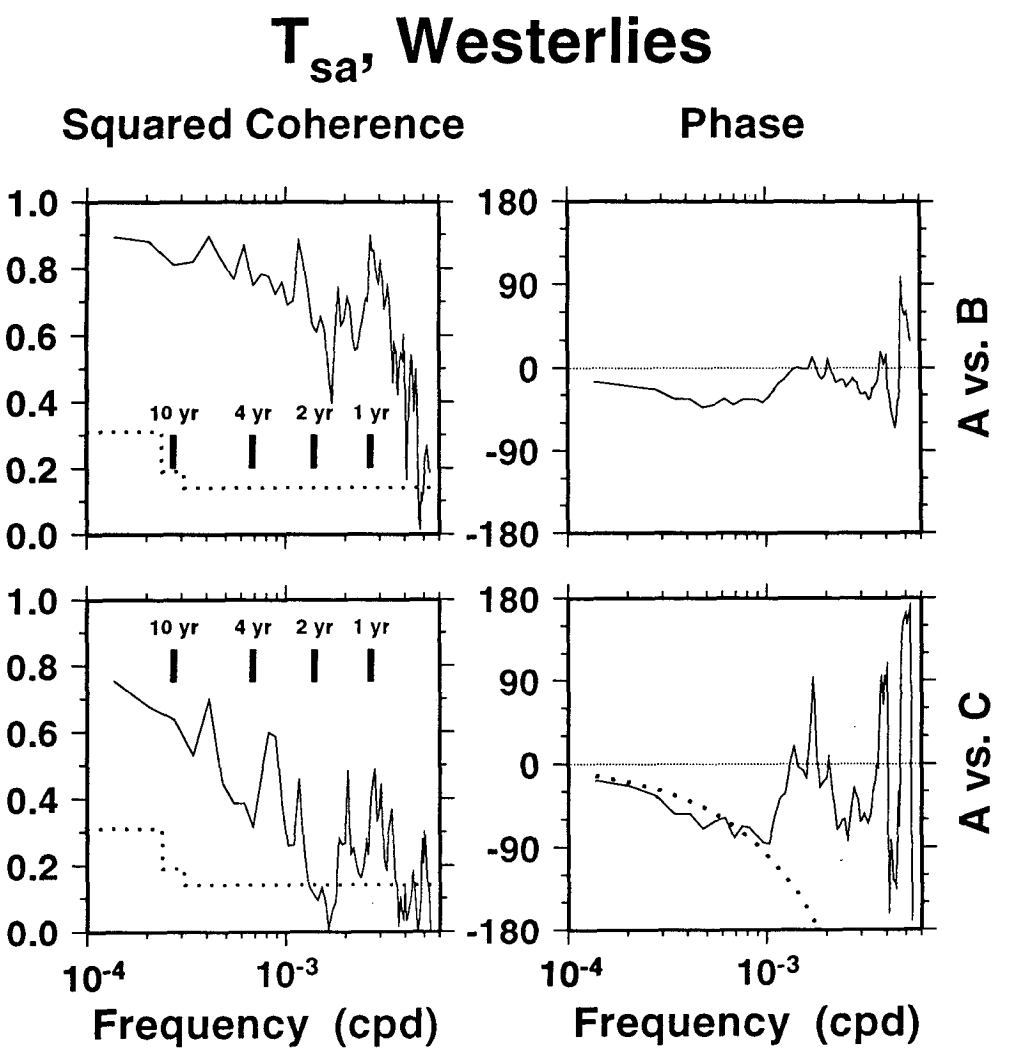

FIG. 3. Squared coherence and phase between T_{sa} fluctuations at point A and point B (top) and between T_{sa} fluctuations at point A and point C (bottom). The location of these three points is shown in Fig. 2. Time series for this cross spectrum analysis were obtained by averaging T_{sa} over 9 × 9 grid boxes centered at points A, B, and C. In the phase plot for point A versus point C, the dotted line gives the phase expected if the T_{sa} signal propagates from point A to point C in 300 days, implying a propagation speed of about 6 km day^{-1}.

these two regions as outlined in Fig. 2. Exact placement of these regions was partly governed by the desire to maximize the positive correlation between $\partial T_{sa}/\partial t$ and F_T so that the response analysis could be conducted with reasonable statistical significance. The large T_{sa} variability in the chosen Westerly wind analysis domain has been a primary focus of the earlier studies that documented the influence of oceanic forcing at decadal and longer periods and of local wind forcing at shorter interannual periods (Bjerknes 1964; Delworth et al. 1993; Kushnir 1994).

The subdomain for the westerlies is restricted to the western part of the basin because the forced T_{sa} response tends to propagate to the east and northeast across the basin. To characterize this propagation, cross-spectrum analysis was performed using T_{sa} time series at three different locations within the westerly wind belt labeled by the points A, B, and C in Fig. 2. Squared coherence and phase plots for point B relative to point A, and also for point C relative to point A, show clear evidence of propagation (Fig. 3). The T_{sa} fluctuations at point B are significantly coherent with those at point A over all periods exceeding 9–10 mo. T_{sa} fluctuations at point C are significantly coherent with those at point A over nearly all periods exceeding 2.5 yr, but only at some shorter periods (primarily near 1 yr). The phase of point C relative to point A reveals that over periods between 2.5 and 20 yr, T_{sa} fluctuations propagate at a characteristic speed of about 6 km day^{-1} (Fig. 3). Since this propagation is observed at the lat-

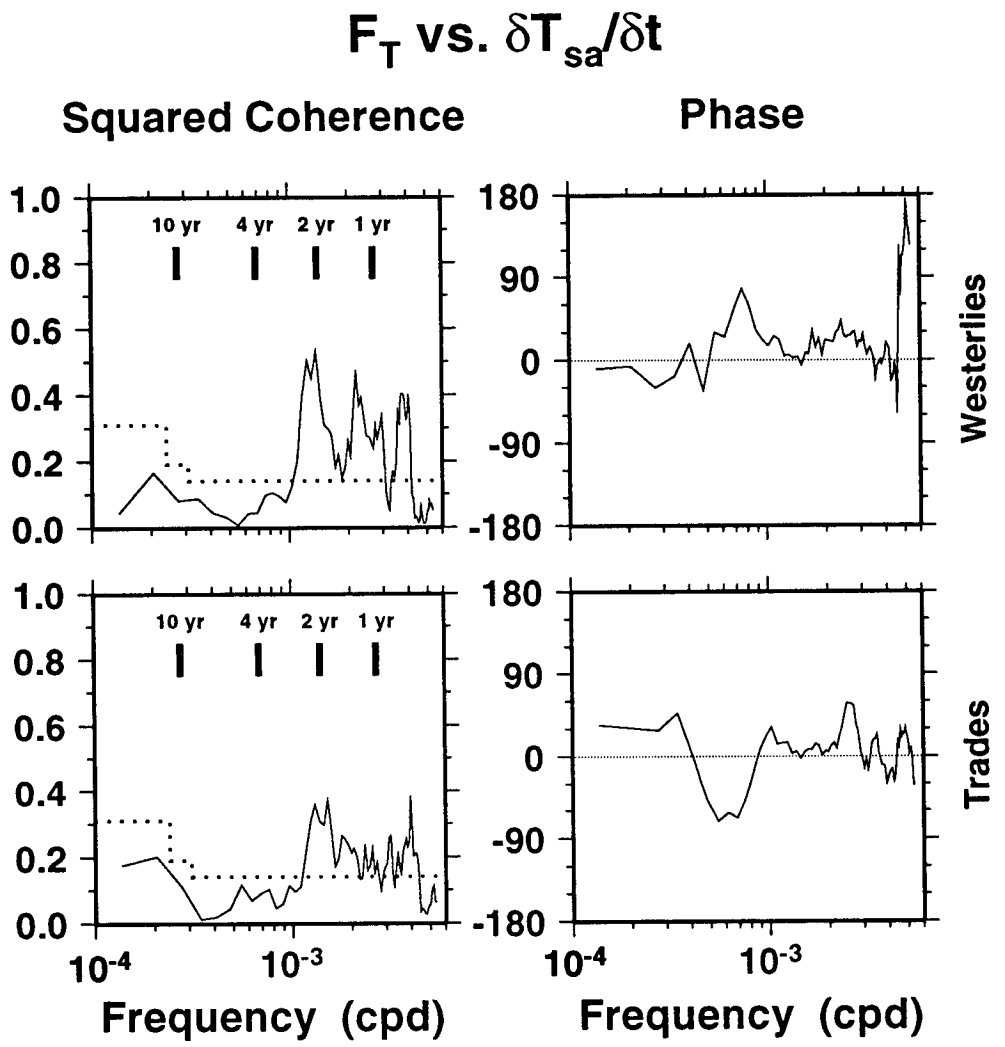

FIG. 4. Squared coherence and phase of $\partial T_{sa}/\partial t$ with respect to F_T in the westerlies (top) and trade winds (bottom). The functions were estimated from autospectrum and cross spectrum estimates calculated at each grid point and ensemble-averaged over the domains shown in Fig. 2. The 95% confidence level is shown for the squared coherence based on band-averaging over three adjacent frequencies at the two lowest frequencies resolved (periods of 20 and 13.3 yr), five adjacent frequencies at the third-lowest frequency resolved (period of 10 yr), and over seven adjacent frequencies at all higher frequencies. Based on estimated spatial correlation scales, approximately 3 degrees of freedom are gained by the spatial ensemble averaging in both analysis domains.

itude of the North Atlantic current, advection by this flow probably contributes significantly to the observed propagation. Similar eastward propagation has been observed in the North Pacific (Michaelsen 1982). Since T_{sa} in the Westerlies is primarily locally forced in the western part of the basin and then propagates away from this region, we restrict our attention to the western basin where local forcing dominates.

4. Local frequency response analysis

a. The importance of decomposing F_T into forcing and feedback components

Although the correlation map between the terms of (11) (Fig. 2) guided the selection of analysis domains, cross-spectrum analysis between these same terms demonstrates the need to decompose F_T into forcing and feedback components. The squared coherence between F_T and $\partial T_{sa}/\partial t$ is statistically significant only over periods between several months and 2.5 yr in both the westerly wind and trade wind analysis domains (Fig. 4). Equation (11) predicts that $\partial T_{sa}/\partial t$ will be in-phase with F_T at all frequencies, and the phase is observed to be near zero at frequencies where coherence is significant (Fig. 4).

It is the insignificant coherence observed at periods exceeding 2.5 yr that underlies the necessity to decompose F_T into forcing and feedback components. At the longer periods resolved in the present study, the lead-

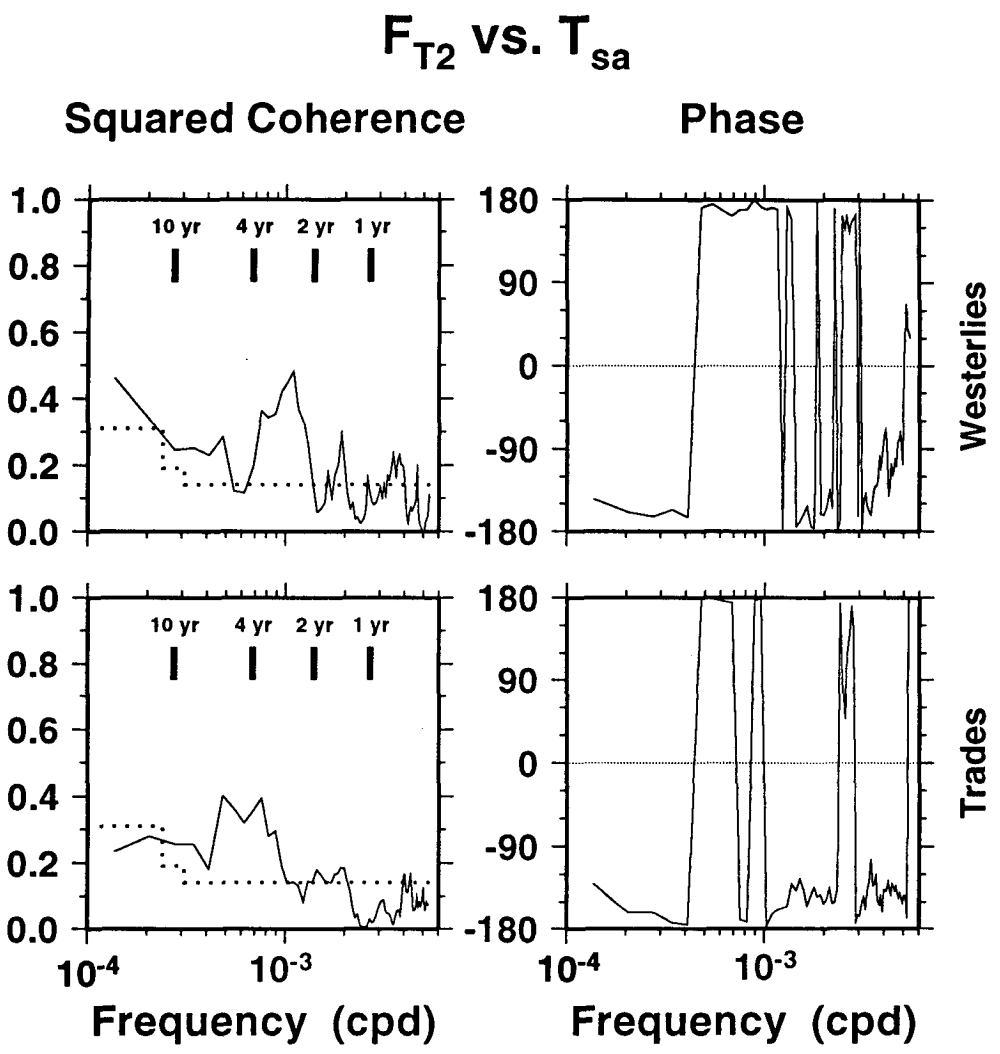

FIG. 5. Squared coherence and phase of T_{sa} with respect to F_{T2} in the westerlies (top) and trade winds (bottom). The functions were estimated from autospectrum and cross spectrum estimates calculated at each grid point and ensemble-averaged over the domains shown in Fig. 2. The 95% confidence level is shown for the squared coherence based on band-averaging over three adjacent frequencies at the two lowest frequencies resolved (periods of 20 and 13.3 yr), five adjacent frequencies at the third-lowest frequency resolved (period of 10 yr), and over seven adjacent frequencies at all higher frequencies. Based on estimated spatial correlation scales, approximately 3 degrees of freedom are gained by the spatial ensemble averaging in both analysis domains.

ing-order balance in (14) becomes $F_{T1} \approx -F_{T2}$. The term $\partial T_{sa}/\partial t$ is therefore of second order and equal to the small residual of the sum of two large terms. At periods exceeding 2.5 yr, (11) represents a balance between two terms with such small magnitude that the signal in the terms estimated from COADS observations is too weak to be detected above the noise. This contention is supported by the subsequent frequency response analysis where it is demonstrated that anomalous surface turbulent heat flux actually does drive a significant fraction of T_{sa} variability at periods exceeding 2.5 yr. The approximate decomposition of F_T into forcing and feedback components was crucial to detecting this longer-period forcing.

b. Does F_{T2} predominantly represent negative feedback damping?

We use cross-spectrum analysis between T_{sa} and F_{T2} to demonstrate that F_{T2} predominantly represents negative linear feedback damping. In both the westerlies and trades, coherence between T_{sa} and F_{T2} is generally larger at periods exceeding about 2 yr in the westerlies and 2.5 yr in the trades than it is at shorter periods (Fig. 5), consistent with the expected greater importance of feedback damping at longer periods. At annual and shorter periods, phase in the westerlies differs substantially from 180° while coherence in the trades tends to be statistically insignificant (Fig. 5). At interannual pe-

riods, T_{sa} is generally close to 180° out of phase with F_{T2} in both the westerlies and trades. Given that this out of phase relationship is predicted by (14c), F_{T2} predominantly represents negative feedback damping at interannual periods.

It must be emphasized that F_{T2} does not exclusively represent negative feedback damping, even at interannual periods. From (14c), the coherence between T_{sa} and F_{T2} would theoretically equal 1.0 if F_{T2} represented only feedback damping. Observed squared coherences (Fig. 5) are substantially smaller than 1.0. Although this reduction in coherence is partly due to noise in the observations used to estimate these fields, part of the reduction likely results because F_{T2} contains substantial variability unrelated to feedback damping such as forcing by T_{Aa} and q_{Aa} variability and the influence of unresolved synoptic variability. Greatbatch et al. (1996, manuscript submitted to *Geophys. Res. Lett.*) detected the influence of atmospheric temperature and humidity on T_{sa} in a global analysis conducted as a function of latitude. Given that (7) predicts a response amplitude that becomes larger with increasing period, present results suggest that forced T_{sa} (and hence q_{sa}) fluctuations become sufficiently large with respect to T_{Aa} and q_{Aa} fluctuations at interannual periods for F_{T2} to predominantly contribute to feedback damping within the westerly wind and trade wind analysis domains. At these longer periods, T_{Aa} and q_{Aa} respond strongly to changes in T_{sa} (and vice versa), so that T_{Aa} and q_{Aa} tend to simply track T_{sa} (and the associated q_{sa}) changes within both analysis domains (e.g., Frankignoul 1985; Battisti et al. 1995). This tracking will not be as tight closer to continents where T_{Aa} and q_{Aa} fluctuations are larger. As a result, F_{T2} may not predominantly act as a negative feedback at interannual periods closer to continents.

c. *Frequency bands where local wind forcing is important*

In the westerlies, T_{sa} is significantly coherent with F_{T1} at nearly all periods between 10 mo and 8 yr, with the largest coherence observed at periods between 2 and 4 yr (Fig. 6). The coherence is very small at decadal and longer periods and also at periods of 6–8 months. About one-half of the observed T_{sa} variance in the 2–4-yr band can be accounted for by the forcing F_{T1} (not shown). In the trades, T_{sa} is significantly coherent with F_{T1} over all periods between 8 mo and 13.3 yr with relatively large coherence observed at periods of 2–3 yr and 7–13.3 yr (Fig. 6). In both the westerlies and trades, a significant response of T_{sa} to local wind forcing F_{T1} is detected at periods exceeding 2.5 yr, which was not possible by analyzing the balance (11).

Insignificant coherence observed at the shortest periods resolved in both the westerlies and trades could indicate that local wind forcing is not as important at these periods. However, it could also result from inadequate sampling in the COADS dataset; that is, estimates of COADS fields for an individual season may be based on very few data points over large regions of the North Atlantic. The insignificant coherence observed at decadal and longer periods in the westerlies is consistent with the Bjerknes (1964) hypothesis to the extent that forcing must be provided by processes other than F_{T1} (oceanic flow?). However, results of the winter-only analysis (section 4e) will cast doubt on this hypothesis.

d. *Analysis of the frequency response function*

Reasonably good agreement exists between the observed and predicted frequency response functions in both the westerlies and trades (Fig. 6). In both regions, the observed gain of T_{sa} relative to F_{T1} has the approximate form of the predicted function (7) over frequencies where coherence is significant. In the westerlies, the observed phase has the approximate form of the predicted function (8) over periods between 10 mo and 8 yr although it is somewhat more positive than predicted at periods between 10 mo and 1.5 yr. Tighter agreement is observed between observed and predicted phase in the trades. The similarities between the observed and predicted frequency response functions not only validate (4) as a reasonable model of locally forced climatic T_{sa} variability but also demonstrate the importance of local wind forcing as represented by F_{T1}. Also, the relatively high coherence between T_{sa} and both F_{T1} and F_{T2} in the 2–4-yr band suggests that the balance (14) is a rather good approximation to the closed anomalous temperature balance within this band.

Although these results demonstrate the importance of local wind forcing, it must be emphasized that this is not the only important forcing mechanism. The potential importance of q_{Aa} and T_{Aa}, especially close to continents and at relatively short periods, has been mentioned. Ekman flow and anomalous entrainment heat flux at the mixed-layer base also contribute to the forcing. The agreement between the observed frequency response properties of T_{sa} with respect to local wind forcing alone may be in part fortuitous. In the westerlies, for example, cooling due to anomalously strong wind speed (anomalously strong westerlies) will tend to occur simultaneously with anomalous cooling due to Ekman flow, due to advection of anomalously dry continental air off the North American continent, and due to anomalously large entrainment of cold water at the mixed-layer base driven by the enhanced wind stirring and cooling (buoyancy flux) at the surface. The tendency for all of these forcing mechanisms to be in-phase allows the observed frequency response function of T_{sa} with respect to local wind forcing alone to resemble the predicted function, in particular the phase from (8). However, the importance of local wind forcing is demonstrated by the fact that the magnitude of the observed gain of T_{sa} with respect to this forcing

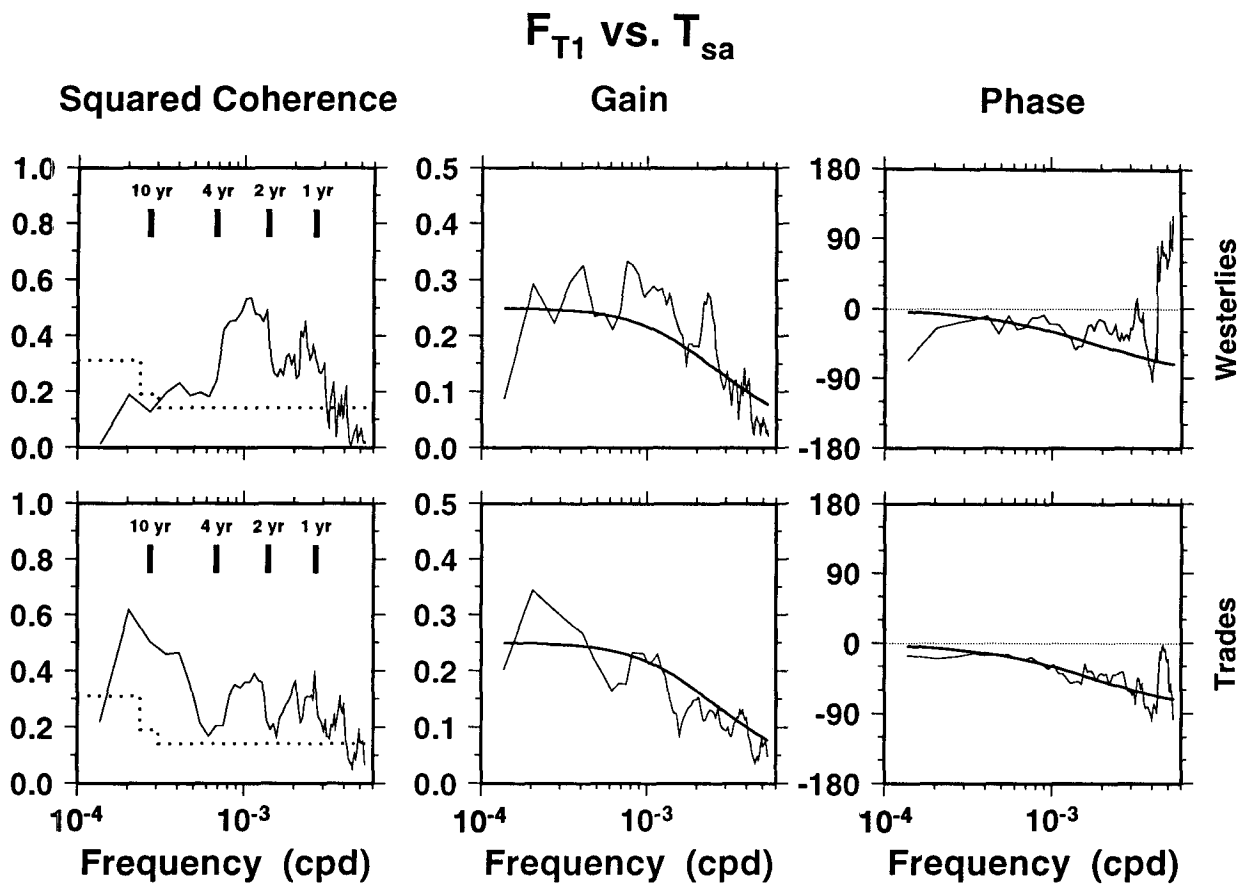

FIG. 6. Squared coherence, gain, and phase of T_{sa} with respect to F_{T1} in the westerlies (top) and trade winds (bottom). The functions were estimated from autospectrum and cross spectrum estimates calculated at each grid point and ensemble-averaged over the domains shown in Fig. 2. Gain and phase functions predicted by (7) and (8) are also shown as the smooth curves. The 95% confidence level is shown for the squared coherence based on band-averaging over three adjacent frequencies at the two lowest frequencies resolved (periods of 20 and 13.3 yr), five adjacent frequencies at the third-lowest frequency resolved (period of 10 yr), and over seven adjacent frequencies at all higher frequencies. Based on estimated spatial correlation scales, approximately 3 degrees of freedom are gained by the spatial ensemble averaging in both analysis domains.

approximately equals the predicted magnitude. Local wind forcing alone is therefore strong enough to drive T_{sa} fluctuations with the observed magnitude and may be the dominant forcing mechanism at some frequencies.

e. Seasonal considerations

To search for seasonal differences in properties of the T_{sa} response, the frequency response analysis was repeated for time series of summer-only and winter-only maps. In general, frequency response properties obtained for a single season do not differ significantly from the results described previously. However, response properties of winter T_{sa} variability in the westerlies differed significantly from results obtained from the full time series analysis. Results of the winter analysis for both the westerlies and trades are now presented to illustrate this point.

In the trade winds, the squared coherence, gain, and phase of T_{sa} with respect to F_{T1} calculated using time series of winter maps (Fig. 7) all show little difference from the functions estimated from the full time series (Fig. 6). In the westerlies, the same is true for the gain and phase functions, but significant coherence extends to much longer periods than was observed for the full time series analysis (Figs. 6 and 7). Although insignificant coherence between the full time series of T_{sa} and F_{T1} at decadal and longer periods in the westerlies is consistent with Bjerknes's (1964) hypothesis, the winter-only results suggest that local wind forcing patterns to a large extent drive the observed winter T_{sa} patterns. Winter T_{sa} variability at decadal and longer periods, and its relationship to anomalous winter atmospheric circulation patterns, has been analyzed in detail in two recent papers (Halliwell 1996a, 1996b, manuscript submitted to *J. Phys. Oceanogr.*). These studies confirm the importance of local wind forcing in

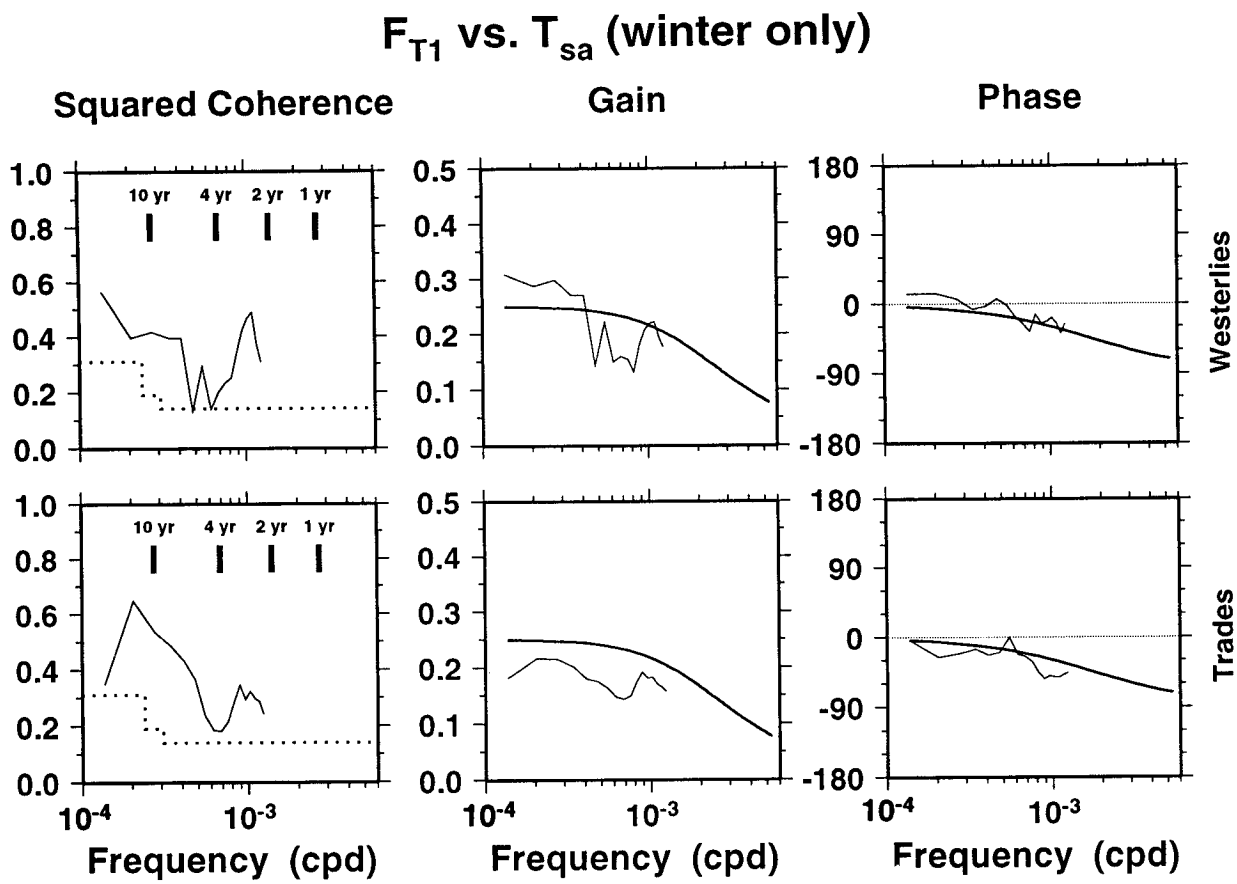

FIG. 7. Same as in Fig. 6, but calculated from time series of the 41 winter-only maps.

driving this winter to winter variability in the westerlies. In contrast, decadal and multidecadal variability of summer T_{sa} in the westerlies is not significantly influenced by local wind forcing, which presumably contributes to the lack of significant coherence observed in the full time series analysis.

5. Discussion

Many studies of T_{sa} variability have related T_{sa} difference, or *tendency,* maps to local atmospheric forcing (e.g., Wallace et al. 1992; Cayan 1992b) under the assumption that local forcing is in-phase with $\partial T_{sa}/\partial t$. Studies relating $\partial T_{sa}/\partial t$ to forcing by anomalous surface heat flux (e.g., Cayan 1992b) have typically used the total anomalous surface turbulent heat flux term of the temperature balance (F_T) to represent the forcing, essentially analyzing the balance (11). These studies were successful because comparisons were made over time scales of a season or shorter where negative feedback damping is relatively unimportant. The frequency response analysis presented here focused on periods between 6 mo and 20 yr and demonstrated that direct comparisons of $\partial T_{sa}/\partial t$ to F_T in (11) were not feasible for variability with periods exceeding about 2.5 yr. Negative feedback damping could not be neglected at these longer periods, the effects of which were to limit the response amplitude and to phase-shift the response so that the forcing was more in-phase with T_{sa} than T_{sa} tendency at these longer periods.

The anomalous surface turbulent heat flux term in the anomalous temperature balance had to be (approximately) decomposed into forcing and negative feedback damping components to obtain these results. Local forcing was specified to be that part of the anomalous surface turbulent heat flux term resulting from local anomalous wind speed (F_{T1}). When F_{T1} was subtracted from F_T, the resulting term (F_{T2}) acted primarily as a negative feedback to dampen T_{sa} variability at interannual periods. With this approximate decomposition of F_T, observed T_{sa} response properties with respect to local anomalous wind speed forcing resembled properties predicted by a simple linearized, first-order anomalous temperature balance, specifically the stochastic model of Frankignoul and Hasselmann (1977) in both the westerly wind and trade wind belts. This resemblance not only indicates that local wind speed is important, but also demonstrates that this highly sim-

plified model provides a good first-order description of the response properties of short-term climatic T_{sa} variability over periods up to at least 20 yr. Although the anomalous mixed-layer temperature balance is complicated and nonlinear, the success of this highly simplified model demonstrates the strong tendency of the mixed layer to integrate the influence of energetic forcing variability. Although the stochastic model can be improved by including the influences of mean advection (e.g., Frankignoul 1985) and seasonal variability in the decay timescale λ^{-1} (Ortiz and de Elvira 1985), the latter resulting largely from seasonal variability in h and the thermal inertia of the mixed layer, these improvements are not necessary to achieve a good first-order description of T_{sa} frequency response properties.

In the westerlies, local anomalous wind forcing through the resulting anomalous surface heat flux is effective over periods between several months and 8 yr, primarily over periods between 2 and 4 yr. Negative feedback damping provided by the anomalous surface heat flux also has a very significant influence on T_{sa} variability in the 2–4-yr band, suggesting that these two terms tend to dominate the temperature balance at these periods. When coherence is computed using the full seasonal time series of F_{T1} and T_{sa}, it is not significant at periods exceeding 8 yr. However, when coherence is computed using a time series of winter-only maps, significant coherence is observed at periods of 8–20 yr. This result suggests that (at least during winter) atmospheric forcing of T_{sa} variability at periods exceeding decadal may be more important than previously realized, a contention that is supported by other recent analyses (Halliwell 1996a, 1996b, manuscript submitted to *J. Phys. Oceanogr.*). This winter T_{sa} response will have to be accurately accounted for to unambiguously identify the winter T_{sa} response to oceanic flow in general, and the MOC in particular, that is known to be important at these longer periods (Bjerknes 1964; Delworth et al. 1993; Kushnir 1994). In contrast to the westerlies, wind forcing in the trades is effective over periods from 8 mo to 13.3 yr, primarily over periods of 2–3 yr and 7–13.3 yr, and did not show strong seasonal differences.

The properties of forced T_{sa} variability described in this paper must be properly simulated by coupled ocean–atmosphere models if they are expected to accurately simulate the climate system. Recent numerical experiments with a simplified coupled ocean–atmosphere system (with the "Atlantic" Ocean represented as a rectangular domain) by O'Brien and Chassignet (1995, manuscript submitted to *J. Climate*) have encouragingly reproduced energetic wind-forced T_{sa} variability in the model westerly and trade wind belts. They used T_{sa} tendency analysis to confirm that the model atmosphere was locally forcing the model ocean. The capability of such coupled models to reproduce the frequency-dependent properties of ocean–atmosphere interaction described here will provide stringent tests of their realism.

Acknowledgments. We gratefully acknowledge the support of the NOAA Atlantic Climate Change Program under Grant number NA90RAH00075. We thank Peter Lamb for providing his Atlantic mixed-layer thickness climatology.

REFERENCES

Battisti, D. S., U. S. Bhatt, and M. A. Alexander, 1995: A modeling study of the interannual variability in the wintertime North Atlantic Ocean. *J. Climate,* **8,** 3067–3083.

Bjerknes, J., 1964: Atlantic air–sea interaction. *Advances in Geophysics,* Vol. 10, Academic Press, 1–82.

Cayan, D. A., 1992a: Latent and sensible heat flux anomalies over the northern oceans: The connection to monthly atmospheric circulation. *J. Climate,* **5,** 354–369.

——, 1992b: Latent and sensible heat flux anomalies over the northern oceans: Driving the sea surface temperature. *J. Phys. Oceanogr.,* **22,** 859–881.

Delworth, T., S. Manabe, and R. J. Stouffer, 1993: Interdecadal variations of the thermohaline circulation in a coupled ocean–atmosphere model. *J. Climate,* **6,** 141–157.

Deser, C., and M. L. Blackmon, 1993: Surface climate variations over the North Atlantic Ocean during winter, 1900–1989. *J. Climate,* **6,** 1743–1753.

Folland, C. K., T. M. Palmer, and D. E. Parker, 1986: Sahel rainfall and worldwide sea temperature. *Nature,* **320,** 602–606.

Frankignoul, C., 1979: Stochastic forcing models of climate variability. *Dyn. Atmos. Ocean,* **3,** 465–479.

——, 1985: Sea surface temperature anomalies, planetary waves, and air–sea feedback in the middle latitudes. *Rev. Geophys.,* **23,** 357–390.

——, 1995: Climate spectra and stochastic climate models. *Analysis of Climate Variability, Application of Statistical Techniques,* H. von Storch and A. Navarra, Eds., Springer-Verlag, 29–51.

——, and K. Hasselmann, 1977: Stochastic climate models. II. Application to sea surface temperature variability and thermocline variability. *Tellus,* **29,** 284–305.

——, and R. W. Reynolds, 1983: Testing a dynamical model for midlatitude sea surface temperature anomalies. *J. Phys. Oceanogr.,* **13,** 1131–1145.

Haney, R. L., 1985: Midlatitude sea surface temperature anomalies: A numerical hindcast. *J. Phys. Oceanogr.,* **15,** 787–799.

Kraus, E. B., 1982: Ocean variability on climate scales. *Progress in Oceanography,* Vol. 11, Pergamon, 61–68.

Kushnir, Y., 1994: Interdecadal variations in North Atlantic sea surface temperature and associated atmospheric conditions. *J. Climate,* **7,** 141–157.

Lamb, P. J., 1984: On the mixed-layer climatology of the north and tropical Atlantic. *Tellus,* **36A,** 292–305.

Lau, N.-C., and M. J. Nath, 1990: A general circulation model study of the atmospheric response to extratropical SST anomalies observed in 1950–79. *J. Climate,* **3,** 965–989.

Luksch, U., and H. von Storch, 1993: Modeling the low-frequency sea surface temperature in the North Pacific. *J. Climate,* **5,** 893–906.

Mayer, D. A., and R. H. Weisberg, 1993: A description of COADS surface meteorological fields and the implied Sverdrup transports for the Atlantic Ocean from 30°S to 60°N. *J. Phys. Oceanogr.,* **23,** 2201–2221.

Michaelsen, J., 1982: A statistical study of large-scale, long-period variability in North Pacific sea surface temperature anomalies. *J. Phys. Oceanogr.,* **12,** 694–703.

Michaud, R., and C. A. Lin, 1992: Monthly summaries of merchant ship surface marine observations and implications for climate variability studies. *Climate Dyn.,* **7,** 45–55.

Ortiz, M. J., and A. R. de Elvira, 1985: A cyclo-stationary model of sea surface temperatures in the Pacific Ocean. *Tellus,* **37A,** 14–23.

Reynolds, R. W., 1979: A stochastic forcing model of sea surface temperature anomalies in the North Pacific and North Atlantic. Rep. 8, 22 pp. [Available from Climate Research Institute, Oregon State University, Corvallis, OR 97331.]

Wallace, J. M., C. Smith, and C. S. Bretherton, 1992: Singular-value decomposition of wintertime sea surface temperature and 500-mb height anomalies. *J. Climate,* **5,** 561–576.

Woodruff, S. D., R. J. Slutz, R. L. Jenne, and P. M. Steurer, 1987: A Comprehensive Ocean–Atmosphere Data Set. *Bull. Amer. Meteor. Soc.,* **68,** 1239–1250.

Zorita, E., V. Kharin, and H. von Storch, 1992: The atmospheric circulation and sea surface temperature in the North Atlantic area in winter: Their interaction and relevance for Iberian precipitation. *J. Climate,* **5,** 1097–1108.